

# Highly Dispersed and Active $\text{ReO}_x$ on Alumina-Modified SBA-15 Silica for 2-Butanol Dehydration

Xiaoyan She, Ja Hun Kwak, Junming Sun, Jianzhi Hu, Mary Y Hu, Chongmin Wang, Charles H.F. Peden, and Yong Wang\*

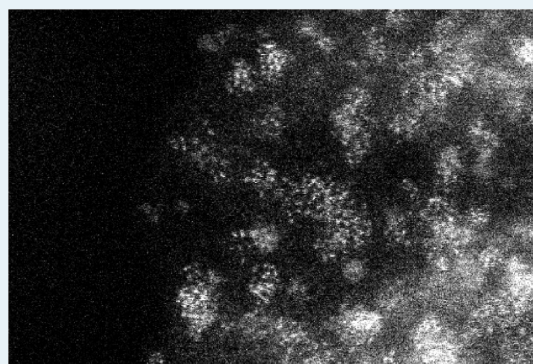
Institute for Integrated Catalysis, Pacific Northwest National Laboratory, Richland, Washington 99352, United States

## Supporting Information

**ABSTRACT:** SBA-15 silica supported rhenium catalysts were synthesized using solution-based atomic layer deposition method, and their activity and stability were studied in the acid-catalyzed 2-butanol dehydration. We find that  $\text{ReO}_x/\text{SBA-15}$  exhibited an extremely high initial activity but a fast deactivation for 2-butanol dehydration at 90–105 °C. Fast deactivation was likely due to the sintering, sublimation, and reduction of rhenia as confirmed by TEM, elemental analysis, and in situ UV–vis (DRS) measurements. To overcome these issues,  $\text{ReO}_x/\text{AlO}_x/\text{SBA-15}$  catalysts with significantly improved stability were prepared by first modifying the surface identity of SBA-15 with alumina followed by dispersion of rhenia using atomic layer deposition. The  $\text{AlO}_x$  phase stabilizes the dispersion of small and uniform rhenia clusters (<2 nm) as confirmed by TEM, STEM, and UV–vis (DRS) characterizations.

Additional  $^{27}\text{Al}$  MAS NMR characterization revealed that modification of the SBA-15 surface with alumina introduces a strong interaction between rhenia and alumina, which consequently improves the stability of supported rhenia catalysts by suppressing the sintering, sublimation, and reduction of rhenia albeit at a moderately reduced initial catalytic dehydration activity.

**KEYWORDS:** rhenia catalyst, catalyst stability, 2-butanol dehydration, SBA-15, in situ UV–vis (DRS), aberration-corrected TEM,  $^{27}\text{Al}$  MAS NMR



## 1. INTRODUCTION

There have been several prior reports of rhenium oxide catalyzed olefin metathesis,<sup>1</sup> partial oxidation/epoxidation,<sup>2–7</sup> hydrogenation,<sup>8–10</sup> reforming,<sup>11–14</sup> hydrodesulfurization (HDS) or HDN (hydrodenitrogenation),<sup>15,16</sup> and  $\text{NH}_3$ –SCR reactions.<sup>17</sup> The catalysis of supported rhenia was reported to be mainly derived from the acidity and redox properties of the rhenium species in these catalysts.<sup>2</sup> For example, reduction of  $\text{Re}^{7+}$  was reported to be essential to form metal-carbene complexes, reported to be the active sites for olefin metathesis.<sup>1</sup> The redox chemistry of rhenia,  $\text{Re}^{6-7+}$  to  $\text{Re}^{4+}$ , has been suggested to play an important role in the selective oxidation of methanol, and also leads to the acidity associated with supported rhenium oxides.<sup>2</sup> The molecular structures of surface rhenium oxide species have been primarily probed by Raman spectroscopy.<sup>4,5,18–23</sup> There seems to be a general agreement in the literature that under dehydrated conditions, tetrahedral (perhaps distorted) surface rhenium oxide exists as monomers with three terminal  $\text{Re}=\text{O}$  bonds and one bond (O-linkage) anchoring Re to the support ( $\text{Re}-\text{O}$ -support), a structure that is independent of the support at low surface coverages. Supported rhenia catalysts have been reported to possess poor stability.<sup>1,24,25</sup> For example, deactivation was reported to be an issue for the rhenia-catalyzed metathesis reaction, a result ascribed to  $\text{H}_2\text{O}$  (impurity) effects, reduction of rhenium, and reductive elimination of intermediates, etc.<sup>1</sup> In addition, surface

rhenium oxide is very volatile via the formation of dimeric  $\text{Re}_2\text{O}_7$  at high temperatures and high surface coverages.<sup>7,20,21</sup>

We have recently reported the preparation of highly dispersed and stable tungsten oxide catalysts supported on mesoporous silica (SBA-15), prepared by a novel solution-based atomic layer deposition (ALD) method, for 2-butanol dehydration.<sup>26,27</sup> Using this same ALD procedure, we have also demonstrated that the surface identity of mesoporous silica can be tailored by adding an extra anchoring phase titania to enhance the dispersion and stability of supported  $\text{VO}_x$  catalysts.<sup>26,28</sup> As the neighbor of tungsten in the periodic table, rhenium oxides may also be of interest for acid catalyzed reactions similar to that of supported tungsten oxides since it has been reported to possess acidity.<sup>2</sup> However, weak interaction of rhenium oxide with  $\text{SiO}_2$  has been well documented in the literature. For instance Edreva–Kardjjeva and Andreev<sup>25</sup> reported rapid deactivation of a  $\text{Re}_2\text{O}_7/\text{SiO}_2$  catalyst in 1-butene metathesis, and attributed this deactivation to the poor stability of active rhenia structures (probably the weakly bound  $\text{Re}-\text{O}-\text{Si}$  linkage) on the  $\text{SiO}_2$  support which can be readily reduced. On the contrary, a stronger bonding of rhenia to  $\gamma\text{-Al}_2\text{O}_3$  supports led to the formation of surface

Received: December 8, 2011

Revised: February 22, 2012

Published: April 18, 2012

aluminum perrhenate,  $\text{Al}(\text{ReO}_4)$  or  $\text{Al}(\text{ReO}_4)_3$ , as evidenced by both leaching and spectroscopy methods.<sup>29,30</sup> Moulijn<sup>31</sup> and Wachs<sup>32</sup> have separately reported that the bonding of Re to oxide supports is in the order:  $\text{Al}_2\text{O}_3 \gg \text{SiO}_2$  based on TPR results. Further, a recent work by Lacheen and Iglesia<sup>4,5</sup> also showed stable activity of a  $\text{ReO}_x/\text{ZSM-5}$  (MFI) catalyst in ethanol partial oxidation, and the active sites were proposed to be  $\text{ReO}_3$  attached onto the Lewis basic oxygen of Si–O–Al in the zeolite supports which has been also observed on the silica–alumina supported tantalum catalysts.<sup>33</sup> In the present work, the efficacy of surface modification of mesoporous silica (SBA-15) by alumina via solution-based ALD in the improvement of rhenium oxide dispersion and stability is demonstrated, and the thus-synthesized rhenium catalysts were examined for 2-butanol dehydration. An alumina layer was used in this work to modify the surface of mesoporous SBA-15 silica followed by dispersion of rhenium on  $\text{AlO}_x/\text{SBA-15}$ . The newly prepared  $\text{ReO}_x/\text{AlO}_x/\text{SBA-15}$  catalyst exhibited high activity and significantly enhanced stability during 2-butanol dehydration. The role of alumina in enhancing the stability of rhenium oxide in  $\text{ReO}_x/\text{AlO}_x/\text{SBA-15}$  was further investigated by TEM, STEM, in situ UV–vis and <sup>27</sup>Al MAS NMR measurements. To our knowledge, there have been no prior reports of supported rhenium oxide catalysts for acid catalyzed dehydration reactions in the open literature.

## 2. EXPERIMENTAL

**2.1. Catalyst Synthesis.** Mesoporous SBA-15 silica was used as a catalyst support because of its high surface area, uniform pore size, and good hydrothermal stability. SBA-15 was prepared according to procedures described elsewhere.<sup>34</sup> The measured surface area of SBA-15 is  $\sim 860 \text{ m}^2/\text{g}$ , and the average pore size is 7 nm after calcination at 500 °C for 4 h.

The SBA-15 supported rhenium oxide catalyst  $\text{ReO}_x/\text{SBA-15}$  was prepared using a solution-based atomic layer deposition (ALD) method.<sup>26,27</sup> Metal chloride ( $\text{ReCl}_5$ , Sigma Aldrich, 99.99%) was used as precursor for rhenium. Briefly, SBA-15 was first dehydrated by refluxing in anhydrous toluene (Aldrich, 99.8%) under an  $\text{N}_2$  atmosphere for 3 h. The metal precursor solutions were prepared by first dissolving the respective metal chloride in toluene (150 mL, at RT) and then adding ethanol (20 mL, Aldrich, anhydrous). The mixture was refluxed in a  $\text{N}_2$  atmosphere until no HCl was formed (detected using a wet pH paper strip), followed by removing unreacted ethanol using Dean–Stark distillation to obtain the dark-brown precursor solutions. Loading of the metal oxide precursors onto SBA-15 was carried out by first mixing the dehydrated SBA-15 in toluene with the metal oxide precursor solution at room temperature, followed by refluxing the mixture in  $\text{N}_2$  overnight. After filtration and washing, the obtained solids were dried in air at 120 °C for 0.5 h, which are denoted as “as-synthesized”. The metal loading of the catalysts was controlled at a monolayer coverage on the SBA-15 surface assuming three Si–OH groups on SBA-15 react with one  $\text{ReCl}_5$  precursor molecule, and taking the surface density of Si–OH on SBA-15 as  $4.0 \text{ Si-OH}/\text{nm}^2$ .<sup>35</sup> Hence, a monolayer  $\text{ReO}_x/\text{SBA-15}$  corresponds to  $\sim 30 \text{ wt } \%$  metal oxides (in the stoichiometry of  $\text{ReO}_3$ ).<sup>27</sup>

A series of catalysts with various coverage of rhenium oxide on alumina modified SBA-15, that is, 25%, 50%, 75%, and 100% of a monolayer, were prepared using a sequential ALD method. First, SBA-15 with a monolayer coverage of alumina ( $\text{AlO}_x/\text{SBA-15}$ ) was prepared using the ALD method described above,

and the monolayer coverage of  $\text{AlO}_x$  was determined similarly by using the ratio of Si–OH:Al = 3:1. The aluminum precursor solution was prepared by dissolving aluminum isopropoxide (Sigma-Aldrich) in toluene without adding ethanol and refluxing. The as-synthesized  $\text{AlO}_x/\text{SBA-15}$  sample was calcined at 400 °C in flowing dry air for 1 h. Then rhenium was deposited onto  $\text{AlO}_x/\text{SBA-15}$  using ALD as described above. The loading of rhenium oxide was again controlled at a target coverage based on the amount of SBA-15 in  $\text{AlO}_x/\text{SBA-15}$  ( $\text{Al}_2\text{O}_3$  loading on  $\text{AlO}_x/\text{SBA-15}$  is  $\sim 6.5 \text{ wt } \%$  and assumed to have a negligible effect on the total surface area).  $\text{ReO}_x/\text{AlO}_x/\text{SBA-15}$  represents the catalyst with monolayer coverage of rhenium oxide, and catalysts with 25%, 50%, and 75% of monolayer coverage are noted separately. All samples were calcined at 400 °C for 1 h in flowing dry air, followed by further calcination in static air at 500 °C for a short time ( $\sim 18 \text{ min}$ ) to remove carbonaceous deposits. Unless otherwise mentioned, the experiments were mainly focused on these 500 °C-calcined samples.

Since it has been reported that rhenium oxide sublimates (as  $\text{Re}_2\text{O}_7$ ) at temperatures of  $\sim 300 \text{ }^\circ\text{C}$ ,<sup>36</sup> elemental analysis by inductively coupled plasma optical emission spectrometry (ICP-OES) was conducted (Galbraith Laboratories, Inc.) for rhenium catalysts, both as-synthesized and calcined, as well as catalysts used for 2-butanol dehydration reaction.

**2.2. Catalytic Activity Measurements.** The catalytic performance for 2-butanol dehydration was measured in a quartz flow reactor (1.0 cm i.d.) at atmospheric pressure. Powder samples were pelletized and then sieved to sizes of 60–100 mesh. Typically, 20 mg catalyst samples were used for the activity testing. All catalyst samples were pretreated in helium at 300 °C for 1 h before the catalytic measurements at target reaction temperatures. The reaction gas composition was controlled at 0.5% 2-butanol–He, by vaporizing liquid 2-butanol (Aldrich, anhydrous, 99.5%) into flowing He (UHP) at ambient temperature and pressure. The experiments were run isothermally to evaluate time-on-stream performances. Reactants and products were analyzed by a gas chromatograph (HP 5890) equipped with a HAYESEP T column and flame ionization and thermal conductivity detectors.

**2.3. Scanning Transmission Electron Microscopy (STEM) and Transmission Electron Microscopy (TEM).** STEM images were recorded on a JEOL 2200 FEF aberration corrected electron microscope (High Temperature Materials Laboratory at Oak Ridge National Laboratory). TEM micrographs of mesoporous silica supported metal oxide catalysts were obtained using a JEOL 2010 high resolution electron microscope, which included an energy-dispersive X-ray (EDX) analyzer for elemental analysis. Powder samples were finely ground and then deposited onto a carbon-coated copper grid.

**2.4. In Situ Diffuse Reflectance (DR) UV–vis.** Diffuse reflectance UV–vis spectra were taken using a Shimadzu UV-2101PC spectrophotometer equipped with an in situ HVC (Harrick) reaction chamber. Powder samples were loaded into the sample holder, and spectra were measured in 200–800 nm region. All samples were first pretreated at 300 °C in He for 1 h, and then the temperature was lowered to the target reaction temperature at which point He was switched to the reaction gas (0.5% 2-butanol–He, 30 mL/min) and in situ UV–vis spectra were taken with time. MgO (99%, Aldrich) was used as a standard for UV–vis measurements. The Kubelka–Munk function,  $F(R)$ , was calculated from the adsorption spectra, and the edge energy was the intercept of an extrapolation of the

low energy rise of the plot of  $[F(R)h\nu]^{1/2}$  against the incident photon energy  $h\nu$ .<sup>37</sup>

**2.5. <sup>27</sup>Al Magic Angle Spinning (MAS) Nuclear Magnetic Resonance (NMR).** The single-pulse <sup>27</sup>Al MAS experiments were performed on a 500 MHz Varian-NMR System spectrometer, corresponding to <sup>27</sup>Al Larmor frequency of 130.32 MHz. A commercial MAS probe with a 4.0 mm pencil type spinner system was used. The sample rotor resembles a commercial rotor except that two solid Kel-F plugs were made in such a manner that they can only be fully inserted into the zirconium cylinder after precooling using liquid nitrogen to seal ~30 mg of samples. The sample spinning rate used for all the measurements was  $15.0 \pm 0.01$  kHz. Al(OH)<sub>3</sub> was used as a reference at 0 ppm that is essentially the same as the common standard of 1.5 M Al(NO<sub>3</sub>)<sub>3</sub> in D<sub>2</sub>O. The pulses angle for acquiring <sup>27</sup>Al spectra was approximately 90°, corresponding to a 1.5 μs pulse width. The full spectral width was 5 MHz. All the spectra were acquired at room temperature using a total of 3000 accumulations for acquiring each spectrum, with a recycle time of 1 s. The spectra from various samples were acquired under identical experimental conditions. The match and tuning conditions of the probe were also made the same from sample to sample using a network analyzer.

### 3. RESULTS AND DISCUSSIONS

#### 3.1. Catalytic Activity of Rhenia Catalysts for 2-Butanol Dehydration.

Figure 1 shows the activity for 2-

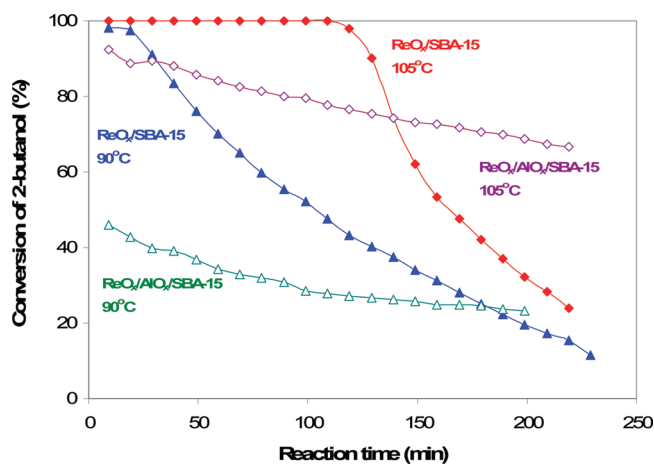


**Figure 1.** Catalytic activity of 2-butanol dehydration over ReO<sub>x</sub>/SBA-15 and ReO<sub>x</sub>/AlO<sub>x</sub>/SBA-15 catalysts. Catalyst amount: 20 mg. Feed gas: 0.5% 2-butanol-He, 200 mL/min.  $T = 90\text{--}105$  °C.

butanol dehydration over ReO<sub>x</sub>/SBA-15 and ReO<sub>x</sub>/AlO<sub>x</sub>/SBA-15 catalysts at 90–105 °C. Three butene isomers (1-butene, *trans*-2-, and *cis*-2-butene) were detected as the major products from 2-butanol dehydration on these rhenium catalysts, similar to 2-butanol dehydration on supported tungsten oxides.<sup>27,38</sup> As shown in Figure 1, at 105 °C, 100% conversion of 2-butanol was obtained over ReO<sub>x</sub>/SBA-15 during the first 120 min TOS, and then the conversion dropped to 23.9% at a TOS of ~220 min, indicating that significant deactivation of ReO<sub>x</sub>/SBA-15 occurred under the 2-butanol dehydration conditions. It should be noted that this deactivation likely also occurred during the first 120 min TOS except that 100% 2-butanol conversion was maintained due to the presence of excess active sites. Because of the extremely high activity of this catalyst at 105 °C, the activity profile was also examined at a lower temperature of 90 °C. At

this temperature, the conversion decreased from ~98% to 11.4% in ~230 min. Therefore, ReO<sub>x</sub>/SBA-15 exhibits a very high initial activity but a fast deactivation for the 2-butanol dehydration reaction.

In contrast to ReO<sub>x</sub>/SBA-15, ReO<sub>x</sub>/AlO<sub>x</sub>/SBA-15 exhibited an improved stability for 2-butanol dehydration, as shown in Figure 1. For example, the conversion level for this alumina-modified catalyst was still 67% at a TOS of ~220 min at 105 °C, as compared to 23.9% for the ReO<sub>x</sub>/SBA-15 catalyst. Similar improvement in catalyst stability was also evident at 90 °C albeit a lower initial activity than that of ReO<sub>x</sub>/SBA-15 (e.g., initial conversions of ~45% vs ~98%). It should be noted that our separate experiments reveal that AlO<sub>x</sub>/SBA-15 (105 °C, at 50 mL/min) and ReO<sub>x</sub>/γ-Al<sub>2</sub>O<sub>3</sub> (Table 1) (90 °C, same

**Table 1. Elemental Composition of ReO<sub>x</sub>/SBA-15 and ReO<sub>x</sub>/AlO<sub>x</sub>/SBA-15 Catalysts**

| samples  | ReO <sub>3</sub> (wt%) | Al <sub>2</sub> O <sub>3</sub> (wt%) | relative rhenia loss in used samples (%) <sup>a</sup> |
|--|------------------------|--------------------------------------|---|
| ReO <sub>x</sub> /SBA-15 (as-syn)                            | 21.5 (±0.12)           |                                      |   |
| ReO <sub>x</sub> /SBA-15 (400 °C-calcined)                   | 18.0 (±0.06)           |                                      | 66.0  |
| ReO <sub>x</sub> /AlO <sub>x</sub> /SBA-15 (as-syn)          | 18.8 (±1.35)           | 4.4 (±0.55)                          |   |
| ReO <sub>x</sub> /AlO <sub>x</sub> /SBA-15 (400 °C-calcined) | 18.1 (±0.12)           | 5.1 (±0.02)                          | 26.0  |
| ReO <sub>x</sub> /γ-Al <sub>2</sub> O <sub>3</sub>           | 4.9 (±0.03)            |                                      | 0   |

<sup>a</sup>After ~3 h 2-butanol dehydration reaction at 90 °C under the same condition as in Figure 1.

condition as in Figure 1) do not exhibit meaningful activity for 2-butanol dehydration with a 2-butanol conversion being less than <1% (data not shown). A further comparison of the reaction rates for the 2-butanol dehydration was conducted for the rhenium catalysts.<sup>27</sup> ReO<sub>x</sub>/γ-Al<sub>2</sub>O<sub>3</sub> catalyst only shows an initial dehydration rate (mol 2-butanol (mol Re)<sup>-1</sup>s<sup>-1</sup>) of  $1.2 \times 10^{-3}$  s<sup>-1</sup> at 90 °C. At the same temperature, for ReO<sub>x</sub>/AlO<sub>x</sub>/SBA-15, the 2-butanol dehydration rate was calculated to be  $15.0 \times 10^{-3}$  s<sup>-1</sup> by using the conversion of 23.1% at ~3 h TOS (Figure 1) and subtracting the amount of sublimated ReO<sub>x</sub> during reaction (Table 1). Therefore, alumina modification of SBA-15 surfaces helps stabilize rhenia catalysts while maintaining its activity, likely because of the interaction of rhenia with the modified support.

**3.2. Characterization of Fresh and Used Catalysts.** As shown in Figure 1, a ReO<sub>x</sub>/SBA-15 catalyst showed a more severe deactivation during 2-butanol dehydration than that of ReO<sub>x</sub>/AlO<sub>x</sub>/SBA-15 which was prepared by modifying the surface of SBA-15 with alumina. To provide an understanding of the role of alumina in mitigating catalyst deactivation, we investigated rhenium sublimation, morphology (e.g., dispersion) changes of supported rhenium oxide before and after reaction by elemental analysis, transmission electron microscopy (TEM) and aberration-corrected scanning transmission electron microscopy (STEM). In situ UV-vis measurements, as a measure of domain size changes during reaction, were also carried out to complement the TEM characterization. <sup>27</sup>Al NMR was employed to provide information on interactions between ReO<sub>x</sub> and AlO<sub>x</sub> in the ReO<sub>x</sub>/AlO<sub>x</sub>/SBA-15 catalyst.

**Elemental Analysis by ICP-OES.** The ICP-OES results for ReO<sub>x</sub>/SBA-15 and ReO<sub>x</sub>/AlO<sub>x</sub>/SBA-15 are shown in Table 1. Comparison of the compositions between the as-synthesized

and calcined catalysts showed that the rhenium sublimation on  $\text{ReO}_x/\text{AlO}_x/\text{SBA-15}$  (from 18.8 wt % to 18.1 wt %) is less than that on  $\text{ReO}_x/\text{SBA-15}$  (from 21.5 wt % to 18.0 wt %) after calcination, suggesting that the modification of SBA-15 with alumina improved the stability of rhenia on  $\text{ReO}_x/\text{AlO}_x/\text{SBA-15}$ . After reaction at 90 °C for 3 h, we noticed that there was a further significant loss of  $\text{ReO}_x$  for  $\text{ReO}_x/\text{SBA-15}$  (66.0% loss) as opposed to a loss of 26.0%  $\text{ReO}_x$  for  $\text{ReO}_x/\text{AlO}_x/\text{SBA-15}$  under the dehydration reaction conditions. It is worth noting that there was no further loss of  $\text{ReO}_x$  for  $\text{ReO}_x/\text{AlO}_x/\text{SBA-15}$  from 3 to 16 h time-on-stream at 90 °C, which further confirms that alumina can be used to improve the stabilization of rhenium oxide on silica support materials.

**TEM/STEM.** Figures 2A and B show TEM micrographs of fresh and used  $\text{ReO}_x/\text{SBA-15}$  catalysts. As can be seen in Figure

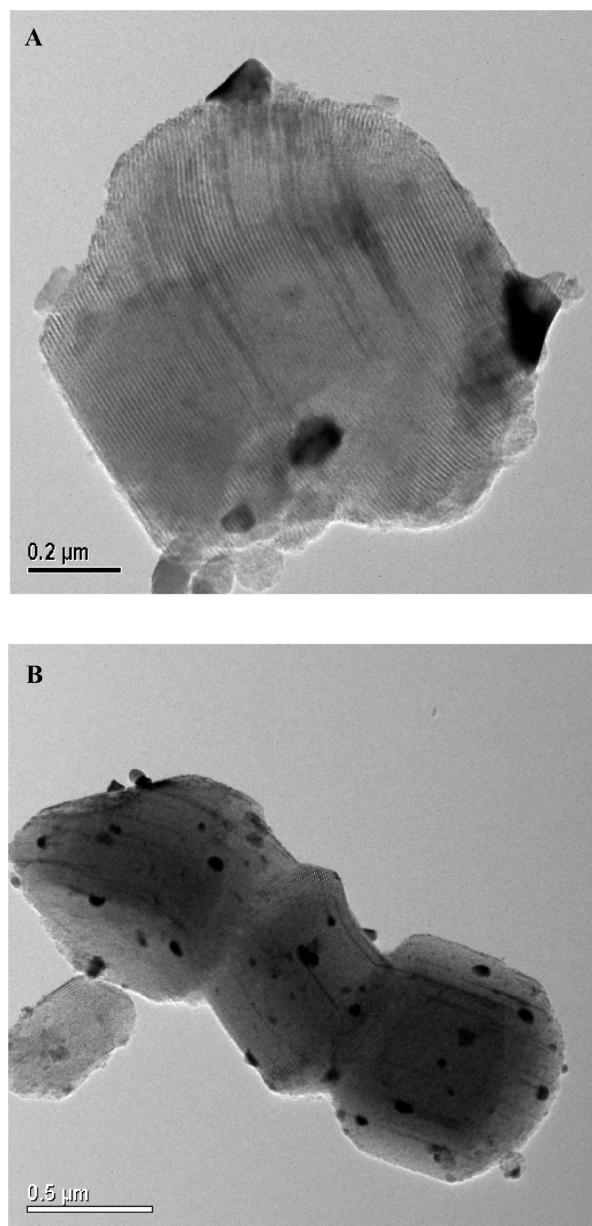


**Figure 2.** TEM micrographs of  $\text{ReO}_x/\text{SBA-15}$ : (A) fresh and (B) after 2-butanol dehydration reaction. Reaction conditions: 0.5% 2-butanol-He, 200 mL/min, 105 °C, and 3.7 h TOS (after reaction for the data shown in Figure 1).

2A, 500 °C-calcination caused partial sintering of rhenia with the appearance of  $\text{ReO}_x$ -particles of  $\sim 100$  nm in diameter. However, these large particles are not abundant which could be due to the fact that majority of rhenia is still well dispersed in the fresh  $\text{ReO}_x/\text{SBA-15}$ , as evidenced by EDX analysis of selected areas without big particles (data not shown) and a very high initial activity (Figure 1). Evident in Figure 2(B), however, is that significant sintering of rhenia took place during reaction for the  $\text{ReO}_x/\text{SBA-15}$  catalyst, leading to a significant increase in the number of rhenia particles of  $\sim 100$  nm in diameter. A parallel elemental analysis (Table 1) indicates that 66.0% of the  $\text{ReO}_x$  was lost during the reaction. The formation of water from 2-butanol dehydration and the presence of large  $\text{ReO}_x$  particles could be the main causes of significant sublimation of active rhenium species via the formation  $\text{Re}_2\text{O}_7$  during the reactions<sup>5</sup> and, thus, the severe deactivation observed for this catalyst.

For the  $\text{ReO}_x/\text{AlO}_x/\text{SBA-15}$  catalyst, which was also calcined at 500 °C, no visible rhenia particles were observed (Figure 3A). An aberration-corrected STEM image (Figure 3B) reveals that very small and uniform rhenia clusters ( $< 2$  nm) exist on the  $\text{AlO}_x/\text{SBA-15}$  support. Especially noteworthy is that most of the small clusters are raftlike, suggesting that rhenia has very strong interactions with the alumina-modified SBA-15 surface, likely suppressing diffusion and, thus, the sintering of rhenium oxide. Furthermore, no rhenia particles were observed in TEM images for the used  $\text{ReO}_x/\text{AlO}_x/\text{SBA-15}$  catalyst (Figure 3C), clearly demonstrating that no significant sintering of rhenia occurred during 2-butanol dehydration. In addition, elemental analysis (Table 1) showed the loss of rhenia in the used  $\text{ReO}_x/\text{AlO}_x/\text{SBA-15}$  is much less than that in the used  $\text{ReO}_x/\text{SBA-15}$  catalyst (26% vs 66%). Even the smaller amount of Re loss observed on  $\text{ReO}_x/\text{AlO}_x/\text{SBA-15}$  could be due to the existence of weakly bounded  $\text{ReO}_x$  similar to  $\text{Re-O-Si}$  in  $\text{ReO}_x/\text{AlO}_x/\text{SBA-15}$  instead of the strongly bounded  $\text{Re-O-Al}$  sites on alumina modified SBA-15 surface. These weakly bounded  $\text{ReO}_x$  ( $\text{Re-O-Si}$ ) could be formed on the exposed SBA-15 surface ( $\text{Si-OH}$ ) since  $\text{AlO}_x$  loading for the  $\text{ReO}_x/\text{AlO}_x/\text{SBA-15}$  sample tested in Figure 1 may still be below the amount to fully cover the SBA-15. Under reaction conditions, these weakly bounded  $\text{ReO}_x$  were lost through sublimation and hence a slight decrease in activity was observed for  $\text{ReO}_x/\text{AlO}_x/\text{SBA-15}$  (Figure 1). It is postulated that this small amount of rhenia loss on  $\text{ReO}_x/\text{AlO}_x/\text{SBA-15}$  can be suppressed by optimizing the  $\text{AlO}_x$  loading, which deserves further investigation.

**In Situ Diffuse Reflectance (DR) UV-vis.** To complement the above-described electron microscopy characterization, in situ UV-vis DRS experiments were conducted to probe changes in rhenia domain size with time during 2-butanol dehydration reaction over  $\text{ReO}_x/\text{SBA-15}$  and  $\text{ReO}_x/\text{AlO}_x/\text{SBA-15}$  catalysts. The average domain size of supported metal oxides can be correlated to the UV-vis absorption edge energy, with smaller domain sizes giving rise to larger edge energies.<sup>39</sup> Such edge energies can be obtained by a Kubelka-Munk function analysis of the diffuse reflectance (DR) UV-vis spectra as described elsewhere,<sup>37</sup> and this method has been widely applied for the investigation of domain size and local structure of supported W-, V-,  $\text{MoO}_x$  catalysts.<sup>37,39,40</sup> Diffuse reflectance UV-vis spectra have also been previously reported for supported rhenium oxides, mainly the  $\text{Re}_2\text{O}_7/\text{Al}_2\text{O}_3$  system,<sup>18,19,41</sup> to suggest the structures of rhenium species in these catalysts.

The in situ UV-vis spectra obtained for  $\text{ReO}_x/\text{SBA-15}$  and  $\text{ReO}_x/\text{AlO}_x/\text{SBA-15}$  during 2-butanol dehydration are shown

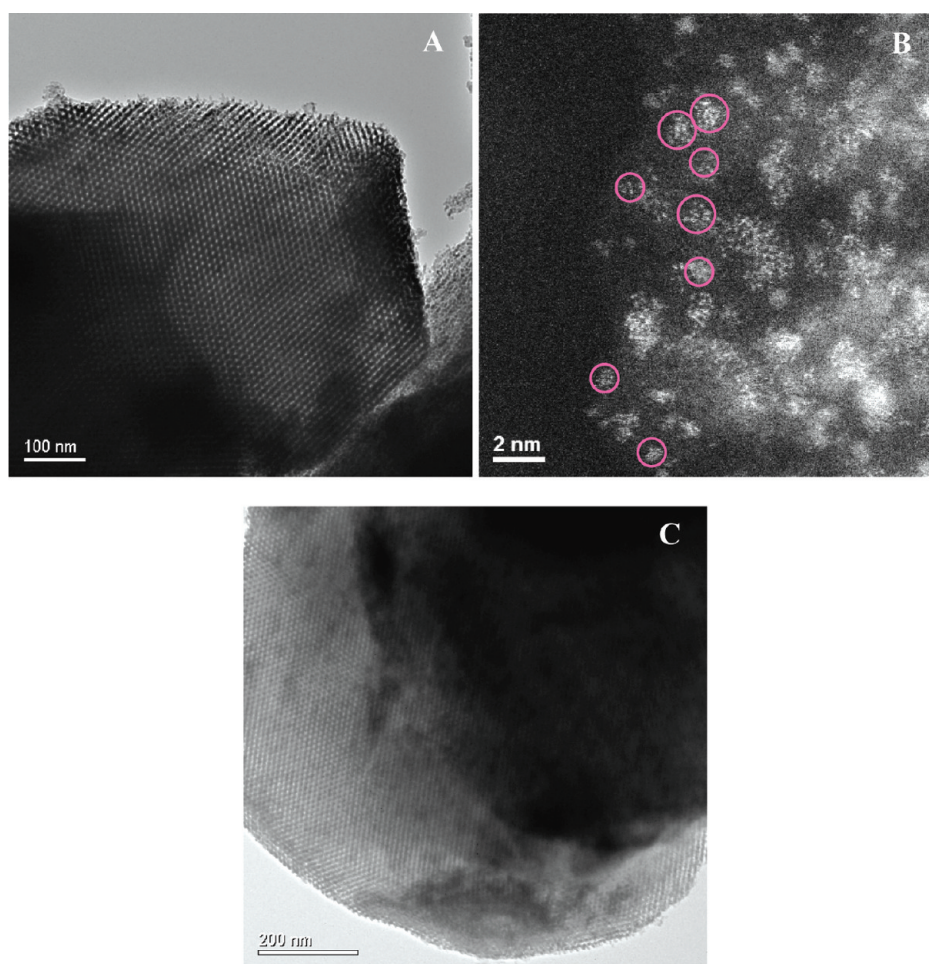


**Figure 3.** TEM micrographs of (A) fresh  $\text{ReO}_x/\text{AlO}_x/\text{SBA-15}$ , (B) HR-STEM micrographs of fresh  $\text{ReO}_x/\text{AlO}_x/\text{SBA-15}$ , and (C) used  $\text{ReO}_x/\text{AlO}_x/\text{SBA-15}$ . For used  $\text{ReO}_x/\text{AlO}_x/\text{SBA-15}$ , reaction conditions: 0.5% 2-butanol-He, 200 mL/min, 105 °C, and 3.7 h TOS (after reaction for the data shown in Figure 1).

in Figures 4A and 4B, respectively. For  $\text{ReO}_x/\text{SBA-15}$  in flowing He at RT, the absorption edge occurs between 310 and 225 nm (4.0–5.5 eV) with calculated  $E_0$  values<sup>37</sup> of  $\sim 4.4$  eV. As the reaction proceeds, however, the spectral edge shifts upward, and consequently, the calculated  $E_0$  values shift to lower values, as shown in Figure 4(C). Within 2 h TOS,  $E_0$  decreased from  $\sim 4.4$  eV to  $\sim 3.9$  eV, indicating the growth of  $\text{ReO}_x$  domain size in  $\text{ReO}_x/\text{SBA-15}$  during 2-butanol dehydration reaction. Thus, the in situ UV–vis experiments further confirm the sintering of rhenia in  $\text{ReO}_x/\text{SBA-15}$  as evidenced by the above-described TEM measurements. In addition, a new pre-edge adsorption feature appeared and increased in intensity with TOS for  $\text{ReO}_x/\text{SBA-15}$ , as shown in Figure 4A, which could indicate that large rhenia clusters are reduced during 2-butanol dehydration, in line with similar observations for supported  $\text{WO}_x$  catalysts during 2-butanol dehydration.<sup>38</sup> The area of the pre-edge absorption peak (open diamonds) and  $E_0$  (filled diamonds) for  $\text{ReO}_x/\text{SBA-15}$  as a function of TOS are shown in Figure 4C. As can be seen in this figure, the pre-edge absorption peak area increased while  $E_0$  decreased with TOS, suggesting that reduction and sintering of rhenia occur during 2-butanol dehydration over  $\text{ReO}_x/\text{SBA-15}$  catalysts, both of which could contribute to the observed catalyst deactivation.

The in situ UV–vis spectra for the  $\text{ReO}_x/\text{AlO}_x/\text{SBA-15}$  catalyst are shown in Figure 4B, with essentially no change in the spectra observed during the 2-butanol dehydration reaction.

The calculated absorption edge energies remained nearly constant at  $\sim 4.5$  eV with TOS as shown in Figure 4C, indicating that there was no rhenia domain size change for this catalyst during 2-butanol dehydration. This result correlates well to the TEM (Figure 3C) and activity (Figure 1) results; that is, stable rhenia dispersion was retained in  $\text{ReO}_x/\text{AlO}_x/\text{SBA-15}$ . Reduction of rhenia was also not observed since the pre-edge absorption peak did not change with TOS (Figure 4B).

The  $E_0$  value for the fresh  $\text{ReO}_x/\text{SBA-15}$  ( $\sim 4.4$  eV) was slightly lower than that of  $\text{ReO}_x/\text{AlO}_x/\text{SBA-15}$  ( $\sim 4.5$  eV), indicating the presence of larger rhenia clusters in the former catalyst, which is consistent with the observed partial sintering of rhenia in the as-calcined  $\text{ReO}_x/\text{SBA-15}$  catalyst (Figure 2A). Similar in situ UV–vis results for 2-butanol dehydration over  $\text{WO}_x/\text{SBA-15}$  have been reported previously,<sup>27</sup> and the domain size of  $\text{WO}_x$  was shown to be stable during reaction, which is also consistent with the stable activity of this catalyst during 2-butanol dehydration.

It is worth noting that Lee and Wachs<sup>23</sup> recently reported edge energy values of  $\sim 4.7$  eV for isolated rhenium oxide supported on  $\text{SiO}_2$  under dehydrated conditions with UV–vis DRS, where the direct-allowed transition was used to calculate  $E_0$  values. Following this methodology, the  $E_0$  of as-calcined  $\text{ReO}_x/\text{SBA-15}$  was recalculated to be of  $\sim 4.8$  eV, which is comparable to Wachs' report, indicating the possible existence

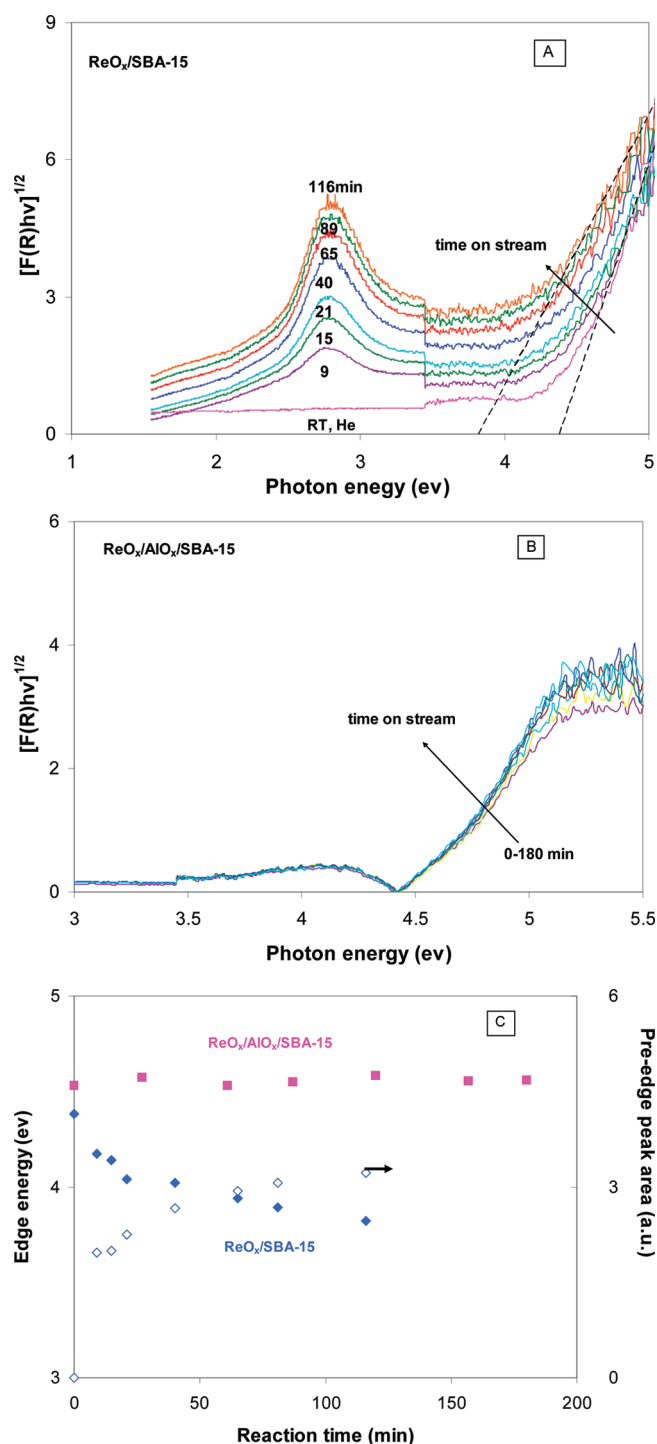


**Figure 4.** In situ UV-vis DRS obtained for (A)  $\text{ReO}_x/\text{SBA-15}$  and (B)  $\text{ReO}_x/\text{AlO}_x/\text{SBA-15}$  catalysts and (C) edge energy ( $E_0$ ) and pre-edge peak area as a function of TOS. Reaction conditions: 105 °C, 0.5% 2-butanol-He, 30 mL/min.

of similar tetrahedral  $\text{ReO}_4$  molecular structures in the  $\text{ReO}_x/\text{SBA-15}$  catalyst prepared using the atomic layer deposition (ALD) method.

**$^{27}\text{Al}$  MAS NMR Spectra.** To further reveal the stabilization of  $\text{ReO}_x$  by  $\text{AlO}_x/\text{SBA-15}$ ,  $^{27}\text{Al}$  MAS NMR was used to characterize a series of  $\text{ReO}_x/\text{AlO}_x/\text{SBA-15}$  samples with different  $\text{ReO}_x$  coverages but a fixed Si/Al ratio as shown in Figure 5. Three peaks centered at 56.0, 30.3, and 0 ppm were clearly observed, which can be assigned to tetrahedrally ( $\text{AlO}_4$ ),

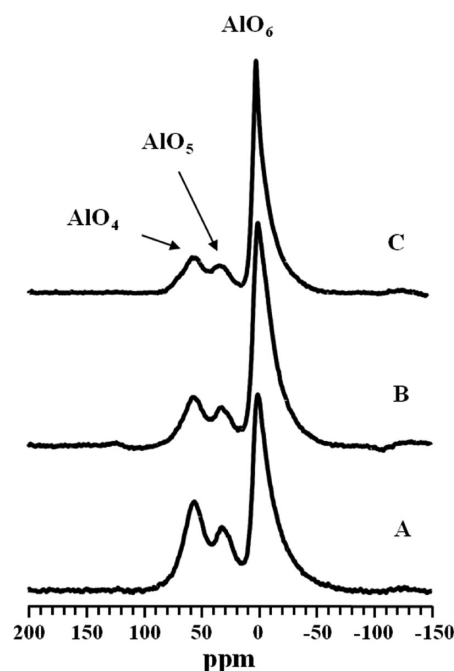


**Figure 5.**  $^{27}\text{Al}$  MAS NMR spectra of  $\text{ReO}_x/\text{AlO}_x/\text{SBA-15}$  samples with Re coverage of (A) 25%; (B) 50%; (C) 75%. Al coverage for all samples is 1.

pentahedrally ( $\text{AlO}_5$ ) and octahedrally ( $\text{AlO}_6$ ) coordinated Al.<sup>42</sup> A careful deconvolution of the spectra has been performed (Supporting Information), and the obtained peak areas representing the corresponding Al species were normalized by the sample weight used for NMR characterization, allowing for a quantification of the different Al species. With increasing  $\text{ReO}_x$  coverage, the amounts of  $\text{AlO}_4$  and  $\text{AlO}_5$  decrease with a concurrent increase of  $\text{AlO}_6$  (Figure 6). This result suggests

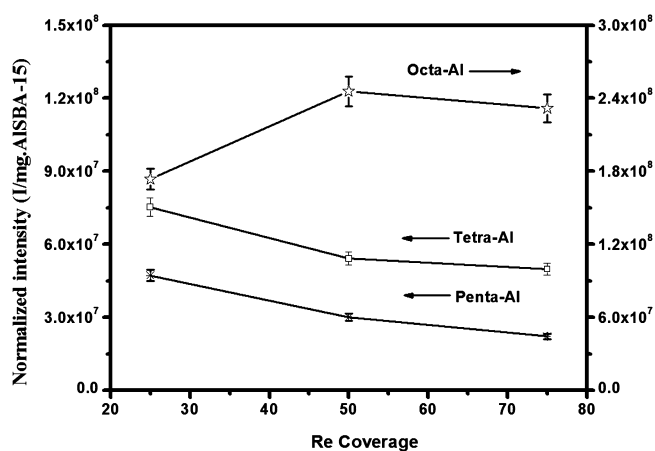


**Figure 6.** Trend of normalized intensity of tetra-, penta-, and octahedral-Al with Re coverage on  $\text{ReO}_x/\text{AlO}_x/\text{SBA-15}$  samples.

that the  $\text{ReO}_x$  species are mainly anchored onto the  $\text{AlO}_4$  and  $\text{AlO}_5$  sites, confirming preferential Re-Al interactions. However, the decrease of signal for  $\text{AlO}_4$  and  $\text{AlO}_5$  is larger than the corresponding increase in  $\text{AlO}_6$  signal. This discrepancy may be due to the formation of paramagnetic  $\text{Re}^{4+}$  centers<sup>43</sup> in the vicinity of Al species, resulting in a loss of  $^{27}\text{Al}$  NMR signal.

## 4. CONCLUSIONS

In this work, we investigated the gas phase 2-butanol dehydration reaction over mesoporous silica (SBA-15) supported rhenia catalysts prepared using a solution-based atomic layer deposition method.  $\text{ReO}_x/\text{SBA-15}$  exhibited a considerably high initial activity but a rapid deactivation in 2-butanol dehydration. The deactivation of the  $\text{ReO}_x/\text{SBA-15}$  catalyst was attributed to significant sintering, sublimation, and reduction of rhenia under the conditions of 2-butanol dehydration as evidenced by TEM, elemental analysis, and in situ UV-vis (DRS) measurements. Modification of the SBA-15 surface identity with alumina enhances the interaction between rhenia and the catalyst support material for the  $\text{ReO}_x/\text{AlO}_x/\text{SBA-15}$  catalyst, which was confirmed by  $^{27}\text{Al}$  MAS NMR. The strong interaction was found to reduce the activity of rhenia but significantly improve the stability of supported rhenia catalysts in 2-butanol dehydration reactions by suppressing its sintering, reduction, as well as sublimation.

## ■ ASSOCIATED CONTENT

### Supporting Information

Deconvolution of  $^{27}\text{Al}$  MAS NMR spectra of  $\text{ReO}_x/\text{AlO}_x/\text{SBA-15}$  samples with various Re coverage. This material is available free of charge via the Internet at <http://pubs.acs.org>.

## ■ AUTHOR INFORMATION

### Corresponding Author

\*E-mail: [yongwang@pnl.gov](mailto:yongwang@pnl.gov).

### Notes

The authors declare no competing financial interest.

## ■ ACKNOWLEDGMENTS

This work was supported by U.S. Department of Energy (DOE), Office of Basic Energy Sciences, Division of Chemical Sciences, Geosciences and Biosciences. The research was performed in the Environmental Molecular Sciences Laboratory, a national scientific user facility sponsored by the DOE Office of Biological and Environmental Research, and located at Pacific Northwest National Laboratory. PNNL is operated for DOE by Battelle. J.S. thanks Liang Zhang (PNNL) for the HR-STEM images recorded at Oak Ridge National Laboratory's High Temperature Materials Laboratory, sponsored by the U.S. Department of Energy, Office of Energy Efficiency and Renewable Energy, Vehicle Technologies Program.

## ■ REFERENCES

- (1) Mol, J. C. *Catal. Today* **1999**, *51*, 289.
- (2) Yuan, Y.; Iwasawa, Y. *J. Phys. Chem. B* **2002**, *106*, 4441.
- (3) Dellamorte, J. C.; Lauterbach, J.; Barteau, M. A. *Catal. Today* **2007**, *120*, 182.
- (4) Lacheen, H. S.; Cordeiro, P. J.; Iglesia, E. *J. Am. Chem. Soc.* **2006**, *128*, 15082.
- (5) Lacheen, H. S.; Cordeiro, P. J.; Iglesia, E. *Chem.—Eur. J.* **2007**, *13*, 3048.
- (6) Liu, J.; Zhan, E.; Cai, W.; Li, J.; Shen, W. *Catal. Lett.* **2008**, *120*, 274.
- (7) Wachs, I. E. *Colloids Surf. A* **1995**, *105*, 143.
- (8) Belousov, V. M.; Palchevskaya, T. A.; Bogutskaya, L. V.; Zyuzya, L. A. *J. Mol. Catal.* **1990**, *60*, 165.
- (9) Enderle, B.; Gates, B. C. *J. Mol. Catal. A: Chem.* **2003**, *204–205*, 473.
- (10) She, X. Y.; Brown, H. M.; Zhang, X.; Ahring, B. K.; Wang, Y. *Chemsuschem* **2011**, *4*, 1071.

- (11) Carvalho, L. S.; Pieck, C. L.; Rangel, M. C.; Figoli, N. S.; Vera, C. R.; Parera, J. M. *Appl. Catal. A-Gen* **2004**, *269*, 105.
- (12) Augustine, S. M.; Sachtler, W. M. H. *J. Catal.* **1989**, *116*, 184.
- (13) Simonetti, D. A.; Kunkes, E. L.; Dumesic, J. A. *J. Catal.* **2007**, *247*, 298.
- (14) Kunkes, E. L.; Simonetti, D. A.; Dumesic, J. A.; Pyrz, W. D.; Murillo, L. E.; Chen, J. G.; Buttrey, D. J. *J. Catal.* **2008**, *260*, 164.
- (15) Pecoraro, T. A.; Chianelli, R. R. *J. Catal.* **1981**, *67*, 430.
- (16) Thomas, R.; van Oers, E. M.; de Beer, V. H. J.; Medema, J.; Moulijn, J. A. *J. Catal.* **1982**, *76*, 241.
- (17) Wachs, I. E.; Deo, G.; Andreini, A.; Vuurman, M. A.; de Boer, M. J. *Catal.* **1996**, *160*, 322.
- (18) Edreva-Kardjjeva, R. M.; Vuurman, M. A.; Mol, J. C. *J. Mol. Catal.* **1992**, *76*, 297.
- (19) Wang, L.; Hall, W. K. *J. Catal.* **1983**, *82*, 177.
- (20) Hardcastle, F. D.; Wachs, I. E.; Horsley, J. A.; Via, G. H. *J. Mol. Catal.* **1988**, *46*, 15.
- (21) Mitra, B.; Gao, X.; Wachs, I. E.; Hirt, A. M.; Deo, G. *Phys. Chem. Chem. Phys.* **2001**, *3*, 1144.
- (22) Lee, E. L.; Wachs, I. E. *J. Phys. Chem. C* **2008**, *112*, 6487.
- (23) Lee, E. L.; Wachs, I. E. *J. Phys. Chem. C* **2007**, *111*, 14410.
- (24) Duquette, L. G.; Cieslinski, R. C.; Jung, C. W.; Garrou, P. E. *J. Catal.* **1984**, *90*, 362.
- (25) Edreva-Kardjjeva, R. M.; Andreev, A. A. *J. Catal.* **1986**, *97*, 321.
- (26) Herrera, J.; Kwak, J.; Hu, J.; Wang, Y.; Peden, C. *Top. Catal.* **2006**, *39*, 245.
- (27) Herrera, J. E.; Kwak, J. H.; Hu, J. Z.; Wang, Y.; Peden, C. H. F.; Macht, J.; Iglesia, E. *J. Catal.* **2006**, *239*, 200.
- (28) Kwak, J. H.; Herrera, J. E.; Hu, J. Z.; Wang, Y.; Peden, C. H. F. *Appl. Catal. A* **2006**, *300*, 109.
- (29) Schekler-Nahama, F.; Clause, O.; Commereuc, D.; Saussey, J. *Appl. Catal. A* **1998**, *167*, 247.
- (30) Okal, J.; Kepinski, L.; Krajczyk, L.; Drozd, M. *J. Catal.* **1999**, *188*, 140.
- (31) Moulijn, J. A.; Mol, J. C. *J. Mol. Catal.* **1988**, *46*, 1.
- (32) Vuurman, M. A.; Stufkens, D. J.; Oskam, A.; Wachs, I. E. *J. Mol. Catal.* **1992**, *76*, 263.
- (33) Sun, J. M.; Chi, M. F.; Lobo-Lapidus, R. J.; Mehraeen, S.; Browning, N. D.; Gates, B. C. *Langmuir* **2009**, *25*, 10754.
- (34) Zhao, D.; Feng, J.; Huo, Q.; Melosh, N.; Fredrickson, G. H.; Chmelka, B. F.; Stucky, G. D. *Science* **1998**, *279*, 548.
- (35) Shenderovich, I. G.; Buntkowsky, G.; Schreiber, A.; Gedat, E.; Sharif, S.; Albrecht, J.; Golubev, N. S.; Findenegg, G. H.; Limbach, H. H. *J. Phys. Chem. B* **2003**, *107*, 11924.
- (36) Arnoldy, P.; van Oers, E. M.; Bruinsma, O. S. L.; de Beer, V. H. J.; Moulijn, J. A. *J. Catal.* **1985**, *93*, 231.
- (37) Barton, D. G.; Shtein, M.; Wilson, R. D.; Soled, S. L.; Iglesia, E. *J. Phys. Chem. B* **1999**, *103*, 630.
- (38) Baertsch, C. D.; Komala, K. T.; Chua, Y.-H.; Iglesia, E. *J. Catal.* **2002**, *205*, 44.
- (39) Weber, R. S. *J. Catal.* **1995**, *151*, 470.
- (40) Gao, X.; Wachs, I. E. *J. Phys. Chem. B* **2000**, *104*, 1261.
- (41) Edreva-Kardjjeva, R. M.; Andreev, A. A. *J. Catal.* **1985**, *94*, 97.
- (42) Li, X. J.; Zhang, W. P.; Liu, S. L.; Xu, L. Y.; Han, X. W.; Bao, X. H. *J. Catal.* **2007**, *250*, 55.
- (43) Yao, H. C.; Shelef, M. J. *Catal.* **1976**, *44*, 392.